Inorganic Chemistry

Article

pubs.acs.org/IC

Heterobimetallic Complexes of Polypyridyl Ligands Containing Paramagnetic Centers: Synthesis and Characterization by IR and EPR

Sarah K. Goforth, Richard C. Walroth, Joseph A. Brannaka, Alexander Angerhofer, and Lisa McElwee-White*

Department of Chemistry, University of Florida, Gainesville, Florida 32611, United States

Supporting Information

ABSTRACT: Ligands containing linked dipicolylamine (dpa) and bipyridine sites have been explored as platforms for the synthesis of heterometallic complexes containing the paramagnetic metals Cu^{2+} and Co^{2+}. IR and EPR studies on the bimetallic complexes and simplified model compounds support dpa-selective binding by both of these metals. The IR spectra have also been compared to those of diamagnetic Rh^{+}, Zn^{2+}, and Pd^{2+} complexes whose metal binding sites had been independently determined through NMR techniques. The binding preferences have been used to control selective metalation in the synthesis of heterometallic Pt/Cu, Pd/Cu, and Rh/Cu complexes.

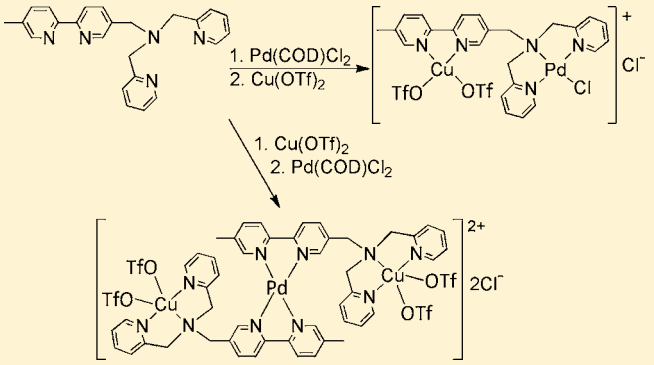

INTRODUCTION

Heterometallic complexes have been synthetic targets because of their potential to act as catalysts with improved or new reactivities compared to their monometallic analogues.[1−6] Controlling the synthesis of well-defined heterometallic complexes can be challenging, and approaches have often involved ligands containing multiple covalently linked multidentate binding sites.[7−15] Because various metals have often been found to display different binding selectivities toward dipicolylamine (dpa) and bipyridine (bpy) when those two moieties are covalently linked,[16−20] we targeted the multisite polypyridyl ligands L1 and L2 as platforms for the synthesis of heterometallic complexes (Figure 1). On the basis of the site selectivities displayed by Rh^{+}, Zn^{2+}, Pd^{2+}, and Pt^{2+} sources, heterometallic Rh/Zn, Rh/Pt, and Rh/Pd complexes were readily produced.[21] In these cases, the metals each had opposing binding selectivities, so the selective synthesis of heterometallic complexes could be achieved by complementary paths in which either metal could be added first (Scheme 1).

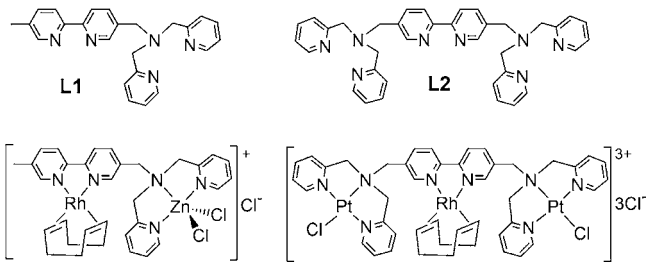

Figure 1. Multisite ligands L1 and L2 and selected diamagnetic heterometallic complexes.

Scheme 1. Complementary Paths for the Formation of Heterometallic Complexes of L1 (or L2) When the Two Metals Have Opposing Binding Selectivities

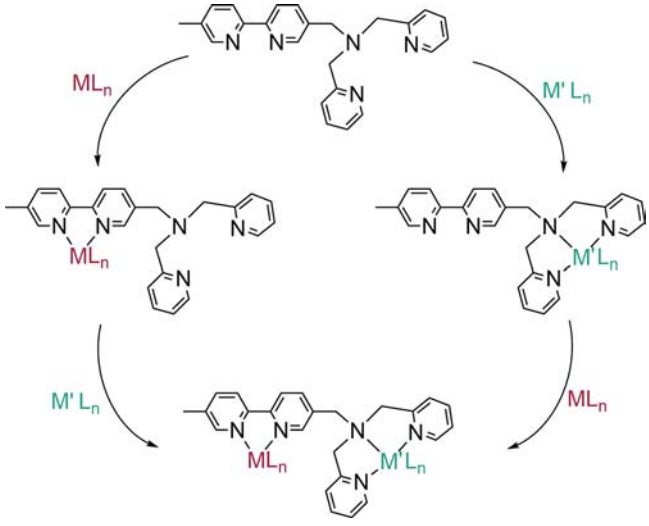

This result is exemplified by bpy-selective Rh^{+} and dpa-selective Pd^{2+}: identical products are formed by either route with retention of both metals at their intrinsically preferred binding sites. Production of L1 and L2 heterometallics by both alternative routes in Scheme 1 will be possible only for certain combinations of metals. If both metals show a preference for the same site (e.g., Zn^{2+}, Pd^{2+}, and Pt^{2+} all prefer dpa binding),

Received: July 27, 2013
Published: November 21, 2013

dx.doi.org/10.1021/ic401952s | Inorg. Chem. 2013, 52, 14116−14123

then only one of the two routes will be accessible. An alternative scheme would apply to the production of heterometallics involving metals with identical dpa-binding preferences and could lead to the selective production of two possible products (Scheme 2, paths a and b) if the metals do not undergo exchange between sites (Scheme 2, paths c and d).

Scheme 2. Possible Formation of Two Different Heterometallic Complexes of L1 (or L2) When the Two Metals Have Identical Binding Selectivities

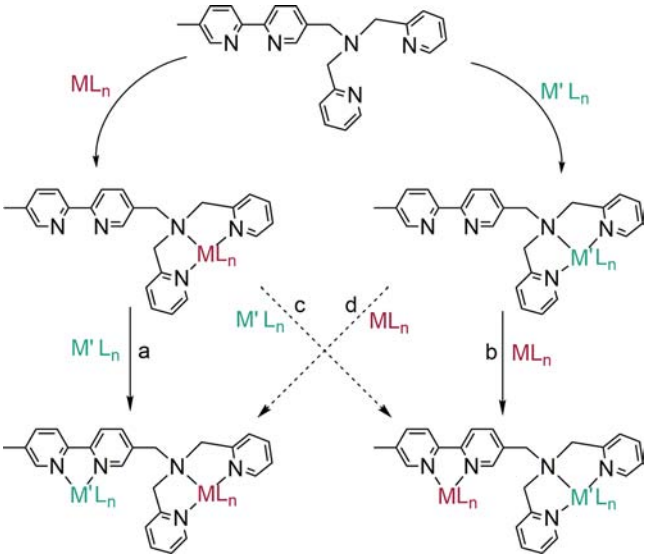

In order to further explore the versatility of L1 and L2 as platforms for heterometallic complexes involving additional metal combinations, we have extended these studies to include Cu and Co. The inclusion of first-row metals in new catalysts is of interest because these metals are cheaper, more readily available, and often more reactive than precious metals such as Rh, Pd, and Pt. In addition, the combination of one of these first-row metals with a precious metal in a heterometallic complex may lead to interesting activity. In particular, Pd/Cu and Pt/Cu heterobimetallic complexes have been targeted in a number of synthetic studies.[9−11,15,22] The motivation behind the Pd/Cu synthetic studies arises from the diverse chemistry of the individual Pd and Cu metals toward small-molecule substrates[10,22] as well as the cooperativity they often display when working together as separate entities as in the Wacker process and in certain Sonagashira coupling reactions.[9] It has been proposed that new reactivities, particularly in the area of oxidation chemistry, might be achieved when Pd and Cu are covalently linked, and heterometallic Pd/Cu complexes have already found some success in early catalytic studies.[9,11] Similar reactivities could be explored for the corresponding Pt/Cu heterometallic complexes. Such complexes may also be useful as model systems for intermediates in the reactions of their Pd/Cu analogues, given the ability of Pt to form stronger bonds than Pd.[10]

We now report identification of the preferred L1 and L2 binding sites of Cu^{2+} and Co^{2+} moieties. The binding-site preference of Cu^{2+} was then exploited in the incorporation of Cu^{2+} into new heterometallic complexes with Rh^{+}, Pd^{2+}, and Pt^{2+}.

EXPERIMENTAL SECTION

General Considerations. Reactions involving Rh complexes were performed using standard Schlenk-line techniques and anhydrous solvents distilled from sodium benzophenone (diethyl ether) or magnesium turnings and I_2 (methanol and ethanol) and stored over 3 Å molecular sieves. All other reactions were performed on the benchtop using solvents obtained from Aldrich or Fisher with no further purification. The $Pd(COD)Cl_2$ was purchased from Strem Chemicals, and all other reagents were obtained from Sigma-Aldrich or Fisher Scientific and used without further purification. $[(PdCl)_2(L2)]Cl_2$, $[(PtCl)_2(L2)]Cl_2$, and [PdCl(L1)]Cl were prepared as described in a previous report.[21] Deuterated solvents were obtained from Cambridge Isotope Laboratories, and ^1H and ^{13}C NMR spectra of ligands were recorded on a Varian 300 MHz Mercury or a Varian 300 MHz Gemini instrument. ^1H NMR signals could not be observed for the paramagnetic complexes. Elemental analyses were performed at Complete Analysis Laboratories in Parsippany, NJ.

Synthesis of Isolated Compounds. *4-[(di-2-picolylamino)-methyl]biphenyl (L1′).* 4-(Bromomethyl)biphenyl (0.534 g, 2.16 mmol), K_2CO_3 (1.192 g, 8.62 mmol), and Bu_4NI (roughly 10 mg) were combined with anhydrous tetrahydrofuran (THF; 40 mL) and dpa (0.58 mL, 3.2 mmol) in a 100 mL Schlenk flask. After stirring at room temperature overnight, the reaction mixture was filtered to remove a tan solid impurity. The solvent of the filtrate was removed to give a brown oil/solid mixture, which was purified by column chromatography on alumina using ethyl acetate as the eluent. The product was collected as a pale-yellow oil (0.683 g, 86%). ^1H NMR (300 MHz, $CDCl_3$): δ 8.53 (d, J = 4.7 Hz, 2H), 7.70−7.30 (m, 13H), 7.10−7.20 (m, 2H), 3.85 (s, 4H), 3.74 (s, 2H). ^{13}C NMR (75 MHz, $CDCl_3$): δ 158.8, 149.0, 141.0, 140.4, 137.3, 137.0, 130.5, 129.7, 129.2, 129.0, 127.9, 127.5, 127.4, 127.3, 127.2, 123.3, 122.5, 59.8, 58.4. Anal. Calcd for $C_{25}H_{23}N_3$: C, 82.16; H, 6.34; N, 11.50. Found: C, 81.80; H, 6.62; N, 11.48. Note: This product slowly develops a yellowish-brown tint while being stored under vacuum but can be used for further synthesis.

5,5′-bis[(dibenzylamino)methyl]-2,2′-bipyridyl (L2″). 5,5′-Bis-(bromomethyl)-2,2′-bipyridyl (0.174 g, 0.510 mmol), K_2CO_3 (0.563, 4.08 mmol), and approximately 10 mg of Bu_4NI were reacted with dibenzylamine (0.24 mL, 1.3 mmol) in anhydrous THF (10 mL) in a 100 mL round-bottom flask. After stirring at room temperature overnight, the yellow mixture became white and was filtered to remove the white solid impurity. The solvent was removed from the filtrate to give another white solid. The crude product was washed with CH_3OH (15 mL) to give the product as a white powder (0.2154 g, 74%). ^1H NMR (300 MHz, $CDCl_3$): δ 8.68 (d, J = 1.6 Hz, 2H), 8.31 (d, J = 8.2 Hz, 2H), 7.82 (dd, J = 8.2 and 2.2 Hz, 2H), 7.45−7.16 (m, 20H), 3.61 (s, 4H), 3.58 (s, 8H). ^{13}C NMR (75 MHz, $CDCl_3$): δ 155.3, 149.9, 139.4, 137.6, 135.2, 129.0, 128.6, 127.3, 120.8, 58.2, 55.2. Anal. Calcd for $C_{40}H_{38}N_4$: C, 83.59; H, 6.66; N, 9.75. Found: C, 83.21; H, 6.81; N, 9.75.

*[Rh(COD)(L1)Cu(OTf)$_2$]Cl (**1**).* Path A: $Cu(OTf)_2$ (0.0174 g, 0.0481 mmol) and L1 (0.0183 g, 0.0480 mmol) were dissolved in ethanol (6 mL) in a 50 mL Schlenk flask and allowed to stir for 15 min. A pale-yellow 17 mL ethanolic solution of $[Rh(COD)Cl]_2$ (0.0118 g, 0.0239 mmol) was then cannula-transferred into the Schlenk flask, resulting in a color change from bright blue to amber brown. After an additional 1.75 h, the solvent was removed and the rust-colored solid was collected (0.0273 g, 58%). Path B: $[Rh(COD)Cl]_2$ (0.0114 g, 0.0231 mmol) and L1 (0.0176 g, 0.0461 mmol) were dissolved in ethanol (7 mL) in a 50 mL Schlenk flask and allowed to stir for 50 min, yielding an orange-red solution. $Cu(OTf)_2$ (0.0167 g, 0.0462 mmol) was cannula-transferred to the reaction Schlenk flask using 16 mL of ethanol, immediately resulting in a brown-red solution. Upon solvent removal in vacuo, the rust-colored product was collected (0.0280 g, 61%). IR/cm^{-1} (neat): 1610 (w), 1574 (vw), 1504 (vw), 1478 (w), 1449 (w), 1413 (vw), 1391 (vw), 1378 (vw), 1245 (s), 1223 (s), 1152 (s), 1101 (w), 1078 (w), 1054 (w), 1027 (s), 1001 (w), 961 (w), 896 (vw), 875 (w), 826 (w), 769 (m), 726 (w), 655 (w). HRMS (ESI-TOF). Calcd for $C_{34}H_{35}ClCuF_6N_5O_6RhS_2$: m/z 839.0447 ([M −

dx.doi.org/10.1021/ic401952s | Inorg. Chem. 2013, 52, 14116−14123

OTf]$^+$). Found: m/z 839.0424. Anal. Calcd for $C_{34}H_{35}ClCuF_6N_5O_6RhS_2$: C, 41.26; H, 3.56; N, 7.08. Found: C, 41.43; H, 3.68; N, 7.16.

[Rh(COD)(L2)(Cu(OTf)$_2$)$_2$]Cl (**2**). Path A: A 2 mL ethanolic solution of $Cu(OTf)_2$ (0.0270 g, 0.0746 mmol) was added to a 2 mL ethanolic solution of L2 (0.0216 g, 0.0373 mmol) in a 50 mL Schlenk flask to give a blue solution. After 15 min, a pale-yellow 15 mL ethanolic solution of $[Rh(COD)Cl]_2$ (0.0092 g, 0.019 mmol) was cannula-transferred into the Schlenk flask, resulting in a color change from bright blue to dark gray. After an additional 1 h, the volume of the dark-brown solution was reduced to less than 5 mL and diethyl ether was added, resulting in precipitation of the product. The supernatant was removed, and the product was washed with 30 mL of diethyl ether and collected as a brown powder (0.0439 g, 76%). Identical IR and electron paramagnetic resonance (EPR) results were obtained when the reaction was performed in methanol. Path B: $[Rh(COD)Cl]_2$ (0.0089 g, 0.018 mmol) and L2 (0.0209 g, 0.0361 mmol) were dissolved in ethanol (8 mL) in a 50 mL Schlenk flask and allowed to stir for 1 h, yielding an orange-red solution. $Cu(OTf)_2$ (0.0261 g, 0.0722 mmol) was cannula-transferred to the reaction Schlenk flask using 2.6 mL of ethanol, which immediately resulted in a dark-brown solution. The product was isolated as in path A to give a brown powder (0.0392 g, 70%). Repeating the reaction in methanol yielded identical results. IR/cm^{-1} (neat): 1612 (w), 1576 (vw), 1479 (w), 1450 (w), 1421 (vw), 1372 (vw), 1358 (vw), 1275 (s), 1242 (s), 1224 (s), 1159 (s), 1102 (w), 1055 (w), 1027 (s), 1003 (w), 961 (w), 896 (vw), 878 (w), 863 (w), 818 (w), 770 (m), 727 (w). Anal. Calcd for $C_{48}H_{46}ClCu_2F_{12}N_8O_{12}RhS_4$: C, 37.23; H, 2.99; N, 7.24. Found: C, 37.07; H, 3.03; N, 7.15.

[Cu(OTf)$_2$(L2)(PdCl)$_2$]Cl$_2$ (**3**). $[(PdCl)_2(L2)]Cl_2$ (0.0214 g, 0.0229 mmol) and $Cu(OTf)_2$ (0.0092 g, 0.025 mmol) were each dissolved separately in 3.8 and 1.7 mL, respectively, of methanol. The $Cu(OTf)_2$ solution was added to the other to give a pale-green solution. The reaction mixture was stirred as a mint-green precipitate formed. The solid was collected by vacuum filtration and washed with diethyl ether to give a mint-green powder (0.0144 g, 49%). IR/cm^{-1} (neat): 1610 (w), 1576 (vw), 1480 (w), 1450 (w), 1412 (vw), 1389 (vw), 1273 (s), 1250 (s), 1223 (s), 1155 (s), 1054 (w), 1029 (s), 937 (w), 904 (vw), 875 (w), 826 (m), 815 (w), 765 (m), 723 (w), 679 (w). HRMS (ESI-TOF). Calcd for $C_{38}H_{34}Cl_4CuF_6N_8O_6Pd_2S_2$: m/z 320.6438 ([M − 2OTf − Cl]$^{3+}$), 1145.8505 ([M − OTf]$^+$). Found: m/z 320.6434, 1145.8529. Anal. Calcd for $C_{38}H_{34}Cl_4CuF_6N_8O_6Pd_2S_2$: C, 35.24; H, 2.65; N, 8.65. Found: C, 35.07; H, 2.60; N, 8.57.

[Cu(OTf)$_2$(L2)(PtCl)$_2$]Cl$_2$ (**4**). A 1.5 mL methanolic solution of $Cu(OTf)_2$ (0.0114 g, 0.0315 mmol) was added to a 7 mL methanolic solution of $[(PtCl)_2(L2)]Cl_2$ (0.0318 g, 0.0286 mmol), resulting in the immediate precipitation of a mint-green solid. After stirring for 15 min, the product was collected by vacuum filtration and washed with 0.7 mL of chilled methanol to give a mint-green powder (0.0261 g, 62%). IR/cm^{-1} (neat): 1615 (w), 1571 (vw), 1480 (w), 1449 (m), 1419 (vw), 1403 (vw), 1392 (vw), 1377 (vw), 1258 (s), 1224 (m), 1153 (s), 1078 (vw), 1059 (w), 1048 (w), 1029 (s), 1011 (w), 969 (w), 955 (w), 933 (w), 898 (vw), 850 (w), 825 (m), 769 (s), 723 (m), 675 (w). HRMS (ESI-TOF). Calcd for $C_{38}H_{34}Cl_4CuF_6N_8O_6Pt_2S_2$: m/z 379.3508 ([M − 2OTf − Cl]$^{3+}$), 417.3453 ([M − OTf − 2Cl]$^{3+}$), 1435.9573 ([M − Cl]$^+$), 700.4942 ([M − 2Cl]$^{2+}$), 586.5106 ([M − 2OTf]$^{2+}$). Found: m/z 379.3505, 417.3451, 1436.9535, 700.4937, 586.5103. Anal. Calcd for $C_{38}H_{34}Cl_4CuF_6N_8O_6Pt_2S_2$: C, 31.00; H, 2.33; N, 7.61. Found: C, 30.92; H, 2.32; N, 7.65.

[Cu(OTf)$_2$(L1)PdCl]Cl (**5**). $Cu(OTf)_2$ (0.0168 g, 0.0464 mmol) was dissolved in 1.5 mL of methanol and added to a 1 mL solution of [PdCl(L1)]Cl (0.0260 g, 0.0465 mmol). The resulting kelly-green solution was reduced to 1 mL in vacuo, and the product precipitated upon the addition of diethyl ether. The deep-mint-green product was collected by vacuum filtration and washed with diethyl ether (0.0320 g, 75%). IR/cm^{-1} (neat): 1611 (w), 1572 (w), 1483 (w), 1450 (w), 1420 (w), 1393 (w), 1376 (w), 1275 (s), 1255 (s), 1225 (s), 1163 (m), 1153 (m), 1112 (w), 1084 (w), 1056 (w), 1031 (s), 938 (w), 900 (w), 865 (w), 824 (w), 770 (m), 722 (w). HRMS (ESI-TOF). Calcd for $C_{26}H_{23}Cl_2CuF_6N_5O_6PdS_2$: m/z 367.9739 ([M − OTf − Cl]$^{2+}$), 770.9167 ([M − OTf]$^+$), 884.9002 ([M − Cl]$^+$). Found: m/z 367.9738, 770.9156, 884.8986. Anal. Calcd for $C_{26}H_{23}Cl_2CuF_6N_5O_6PdS_2$: C, 33.93; H, 2.52; N, 7.61. Found: C, 34.07; H, 2.48; N, 7.58.

[Pd(L1)$_2$(Cu(OTf)$_2$)$_2$]Cl$_2$ (**6**). L1 (0.0251 g, 0.0658 mmol) was dissolved in 2 mL of methanol and reacted with a 2 mL methanolic solution of $Cu(OTf)_2$ (0.0238 g, 0.0658 mmol), resulting in a dark-blue solution. Upon the addition of $Pd(COD)Cl_2$ (0.0188 g, 0.0659 mmol) dissolved in 5 mL of methanol, the reaction solution became turquoise-teal. A fine precipitate began to form within 5 min and was collected by filtration after 4 h. The grayish-teal powder was washed with diethyl ether (0.0254 g, 42%). IR/cm^{-1} (neat): 1611 (m), 1575 (w), 1475 (m), 1449 (m), 1413 (w), 1389 (vw), 1354 (vw), 1364 (vw), 1254 (s), 1224 (m), 1153 (s), 1100 (w), 1084 (w), 1056 (m), 1029 (s), 1001 (w), 965 (w), 945 (w), 931 (w), 900 (w), 879 (w), 844 (m), 817 (m), 769 (m), 761 (m), 708 (w), 684 (w), 656 (m). HRMS (ESI-TOF). Calcd for $C_{52}H_{46}Cl_2Cu_2F_{12}N_{10}O_{12}PdS_4$: m/z 310.9821 ([M − L1 − Cu − 4OTf]$^{2+}$), 367.9739 ([M − L1 − Cu − 3OTf − Cl]$^{2+}$), 770.9167 ([M − L1 − Cu − 3OTf]$^+$). Found: m/z 310.9822, 367.9748, 770.9161. Anal. Calcd for $C_{52}H_{46}Cl_2Cu_2F_{12}N_{10}O_{12}PdS_4$: C, 37.54; H, 2.79; N, 8.42. Found: C, 37.89; H, 2.48; N, 8.76.

IR Studies. All IR data were collected using a Perkin-Elmer Spectrum One FT-IR spectrometer. IR spectra for the Pd complexes were recorded for the products after purification. All reactions involving $Cu(OTf)_2$, $Cu(NO_3)_2$, $CoCl_2$, and $Zn(NO_3)_2$ were conducted in an ambient atmosphere, and no purification steps were taken prior to collection of the IR spectra. In each case, the metal reagent and ligand were dissolved in separate solutions in methanol or acetonitrile. The metal reagent solution was then added dropwise to the stirring ligand solution and allowed to stir for ≈30 min before the solvent was removed, and the IR spectrum was recorded for the solid product.

EPR Studies. Continuous-wave X-band (9.62 GHz) measurements were recorded using a Bruker Elexsys E580 spectrometer equipped with an Oxford ESR900 cryostat set at 20 K. This temperature was used because it offered the best compromise between large Boltzmann population for larger EPR signals and short relaxation times to avoid saturation effects. Experiments were performed either with the standard rectangular TE102 cavity (Bruker ER4102ST) or with the Bruker ER4116DM dual-mode resonator. Neat methanol and 50:50 dimethyl sulfoxide (DMSO)/H_2O were chosen as solvents because of their tendency to form glasses at cryogenic temperatures.[23,24] Samples were prepared in their respective solvents, and approximately 200 μL was transferred into 4 × 5 mm (i.d. × o.d.) quartz tubes. The tubes were then capped and the samples quickly frozen by plunging into liquid nitrogen before they were placed in the precooled cryostat. The methanol used in these studies was dried over 3 Å molecular sieves. DMSO was purchased from Fisher and used without further purification. Deionized water was also used without further purification. Samples of the ligands bpy0, dpa, L2′, L1, and L2 with varying ratios of $Cu(OTf)_2$ were prepared in both methanol (1.0 mM) and 50:50 DMSO/H_2O (1.4 mM) from appropriate stock solutions of the starting materials. Isolated Rh/Cu complexes **1** and **2** were dissolved in methanol (1.0 mM), while Pd/Cu and Pt/Cu samples **3**–**7** were dissolved in 50:50 DMSO/H_2O (1.4 mM). Simulations of the spectra were performed using *EasySpin* in order to determine the EPR parameters.[25]

RESULTS AND DISCUSSION

Cu and Co Binding-Site Preferences for L1 and L2. On the basis of the UV–visible studies of Shinkai and Takeuchi in which $Cu(ClO_4)_2$ was found to bind preferentially to the dpa sites of similar ligands, it was likely that other Cu^{2+} sources would have the same binding preferences in L1 and L2.[16,17] In contrast, the binding preferences of Co in similar ligands had not been explored. For the Rh^+, Pt^{2+}, Pd^{2+}, and Zn^{2+} complexes of L1 and L2, NMR was the primary means of binding-site determination.[21] Unfortunately, the preparation of diamagnetic

Co^{3+} complexes was problematic because Co^{3+} reagents are inert and are also often not soluble in the same solvents as L1 and L2. Although NMR spectra of Co^{2+} complexes are known,[26,27] they do not contain detailed splitting patterns such as those that were useful in assigning the diamagnetic systems. Additionally, UV−visible studies analogous to those of Shinkai and Takeuchi employing Co^{2+} sources were inconclusive. We thus needed to employ another technique in order to determine the binding-site preferences of paramagnetic Co^{2+}.

The initial indication that $CoCl_2$ preferentially binds at the dpa site was gleaned from the physical properties of the $CoCl_2$ complexes of ligands L1 and L2 and their ligand models L1′, L2′, bpy0, and L2″ (Figure 2). All of these ligands, except the

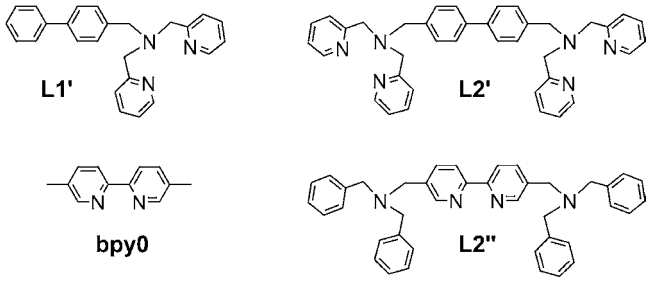

Figure 2. Ligand models containing only one type of binding site.

commercially available bpy0, were prepared in the same manner as the previously reported ligands L1, L2, and L2′ by substitution of dpa onto the appropriate (bromomethyl)-bipyridine or biphenyl derivative.[18,28,29] L1′ and L2′ lack the bpy binding site, while L2″ has no dpa moiety. In contrast to the turquoise precipitates that resulted from reactions of $CoCl_2$ with bpy0 or L2″ (λ_{max} = 587 nm; λ_{max} = 682 nm in CH_3CN), all reactions of $CoCl_2$ with L1, L2, L1′, and L2′ produced purple products (λ_{max} = 560 nm; λ_{max} = 628 nm in CH_3CN). Additionally, the turquoise bpy0 complex displayed little or no solubility in all common organic solvents, while in every case but that of L2, the purple complexes were very soluble in CH_3CN and CH_3OH.

IR Studies of Co and Cu Complexes. Although the similarity of the physical properties is evidence for dpa binding selectivity by $CoCl_2$, additional support was found through a series of IR studies. Upon comparison, the spectra of L1 and L2 undergo qualitatively similar changes when the ratio of $CoCl_2$ added to L1 versus $CoCl_2$ added to L2 is 1:2 (Figure 3). Because there is a 1:2 ratio of dpa sites in L1 to dpa sites in L2, these results suggest that binding is occurring at the dpa site. If binding occurred at the bpy site, there should be more similarities between the spectra of L1 and L2 each with 1 equiv of $CoCl_2$ added. The same series of $CoCl_2$ additions was performed with L2′ as the ligand, and the resulting spectral changes matched very well with those of the L2 study. Similar studies performed with $Cu(OTf)_2$ and $Cu(NO_3)_2$ gave analogous results.

The region between 1440 and 1620 cm^{-1} maintained a consistent profile for the final products resulting from reactions with each of these three reagents. This region of the IR spectra, associated with vibrations involving the pyridine rings,[30−32] was therefore identified as a marker for determining whether or not binding occurred at the dpa site (Figure 4). Specifically, each spectrum contained a major peak between 1606 and 1613 cm^{-1}, a much smaller peak between 1571 and 1576 cm^{-1}, and two broad peaks of approximately equal or lesser intensity than

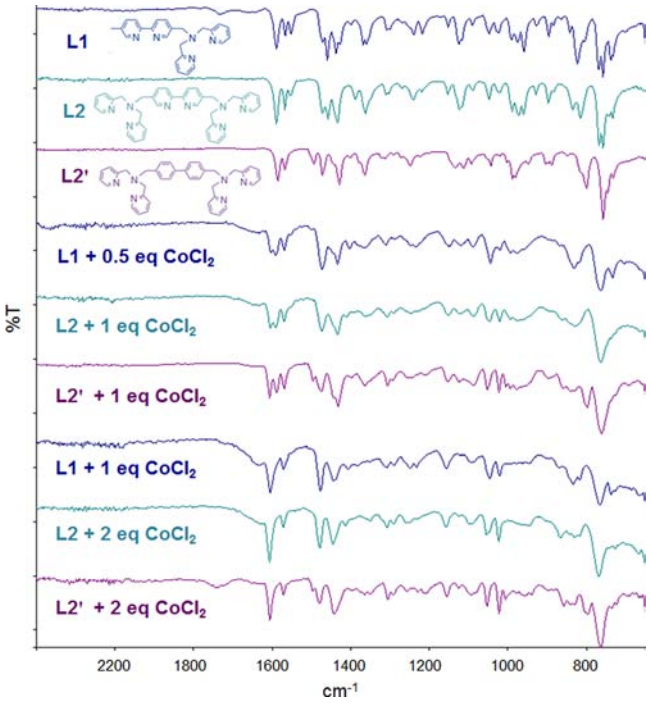

Figure 3. IR study of the addition of $CoCl_2$ to L1, L2, and L2′.

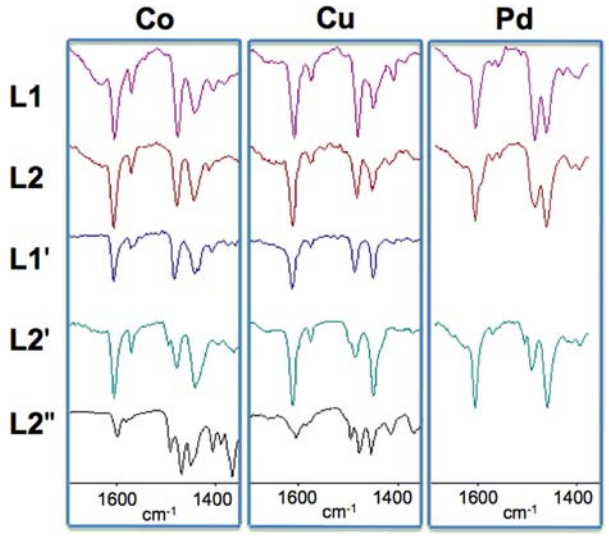

Figure 4. Expansion of the 1400−1600 cm^{-1} region of the IR spectra of L1, L2, L1′, L2′, and L2″ bound to PdCl, $CoCl_2$, or $Cu(OTf)_2$. In all spectra involving L1, L2, L1′, or L2′, the equivalents of metal match the number of dpa sites. One equiv of metal is present in the L2″ cases.

the first between 1478 and 1487 cm^{-1} and between 1444 and 1451 cm^{-1}. The same IR profile was observed in this region for the products of reactions of the ligands with $Pd(COD)Cl_2$ and $Zn(NO_3)_2$, which are both independently known to bind at the dpa site based on NMR studies.[21]

The IR profiles of L2″ complexes of Co and Cu, which must involve bpy binding, are distinctly different from those of their dpa-bound counterparts. Instead of the strong peak associated with C=C stretching between 1609 and 1613 cm^{-1} found in the dpa-bound Cu complexes, a much weaker peak is observed at 1604 cm^{-1}. Similarly, the L2″ complex of Co contains the weaker peak at 1600 cm^{-1} in place of the peak between 1606

dx.doi.org/10.1021/ic401952s | Inorg. Chem. 2013, 52, 14116−14123

and 1607 cm^{-1} observed in the dpa-bound Co complexes. These findings are consistent with other reported asymmetric C═C stretches for dpa and bpy complexes.[30−33] Additionally, the L2″ complexes display three medium or strong peaks in the 1450−1500 cm^{-1} region as opposed to the two generally observed in the dpa-bound complexes.

EPR Studies of Cu Complexes. Because the L1 and L2 binding preference of these Cu^{2+} sources is confirmed to be the dpa site (as also seen for Pt^{2+} and Pd^{2+}), reactions to form Pd/Cu or Pt/Cu complexes could potentially form mixtures of products because of competition between the two metals for the same site. Therefore, sufficient characterization of Pd/Cu and Pt/Cu complexes requires a means of confirming the final binding sites of the two metals. UV−visible or IR studies are not practical for distinguishing between the final placement of either of the two different metals in their heterometallic complexes. In contrast, EPR allows for specific characterization of the environment around the Cu^{2+} center alone, and relatively small changes in this environment can have a measurable effect on the hyperfine structure and *g*-factor anisotropy of the associated Cu^{2+} EPR.

In order to first identify whether or not EPR could be utilized to make this distinction between Cu^{2+} binding at the bpy and dpa sites of L1 and L2, EPR spectra were obtained for various mixtures of ligands with $Cu(OTf)_2$ in CH_3OH and in 50:50 DMSO/H_2O in frozen glasses at 20 K. Because the spectra of mixtures of L1, L2, and L2′ with ratios of Cu^{2+} equal to the number of available dpa sites were very broad, EPR parameters were obtained for mixtures involving half those ratios. The broadening may be relaxational in nature because of lower-quality glasses or increased contact between Cu^{2+} centers at higher concentrations. It is also possible that, at concentrations of Cu^{2+} approaching stoichiometric equivalents relative to the number of dpa sites, there are small populations of bimetallic and trimetallic Cu^{2+} complexes of L1 and L2, respectively. For the ligand models bpy and dpa, $Cu(OTf)_2$ was added in a 1:1 ratio. These EPR spectra were of an axial type (Table 1), as expected based on the literature results for dpa- and bpy-bound Cu^{II} complexes.[34,35] There was no variation in the $g_\perp$ values obtained for the complexes in either solvent. However, in DMSO/H_2O, EPR parameters for the parallel region of dpa and dpa-bound L2′ complexes are significantly different from those for bpy complexes. Because parameters for L1 and L2 most closely match those of the dpa-bound controls, dpa binding selectivity is supported. This comparison can be easily observed with visual inspection of the spectra for L1 and L2, which correspond with that of L2′ but not with that of bpy0 (Figure 5a−d). Although the $g_\parallel$ values obtained for all of the complexes in CH_3OH were essentially the same, the $A_\parallel$ coupling constants showed a trend similar to that observed in the DMSO/H_2O cases.

Table 1. EPR Data Obtained from Mixtures of $Cu(OTf)_2$ and Various Ligands at 20 K

entry	ligand[a]	solvent	$g_\parallel$	$g_\perp$	$A_\parallel$ ($\times 10^{-4}$ cm^{-1})
1		DMSO/H_2O[b]	2.42	2.08	130
2	bpy0	DMSO/H_2O[c]	2.31	2.07	163
3	dpa	DMSO/H_2O[c]	2.26	2.05	179
4	L2′	DMSO/H_2O[c]	2.25	2.07	177
5	L1	DMSO/H_2O[c]	2.27	2.08	187
6	L2	DMSO/H_2O[c]	2.25	2.06	183
7		CH_3OH[d]	2.43	2.09	122
8	bpy0	CH_3OH[e]	2.27	2.06	162
9	dpa	CH_3OH[e]	2.26	2.05	177
10	L2′	CH_3OH[e]	2.27	2.06	173
11	L1	CH_3OH[e]	2.24	2.06	185
12	L2	CH_3OH[e]	2.24	2.06	183

[a]For solutions involving bpy0, dpa, L2′, or L2, the ratio of ligand to Cu^{2+} was 1:1. For the solutions involving L1, the ratio was 1:1.5. [b]50:50 DMSO/H_2O, 1.44 mM in $Cu(OTf)_2$. [c]50:50 DMSO/H_2O, 1.44 mM in ligand. [d]1.0 mM in $Cu(OTf)_2$. [e]1.0 mM in ligand.

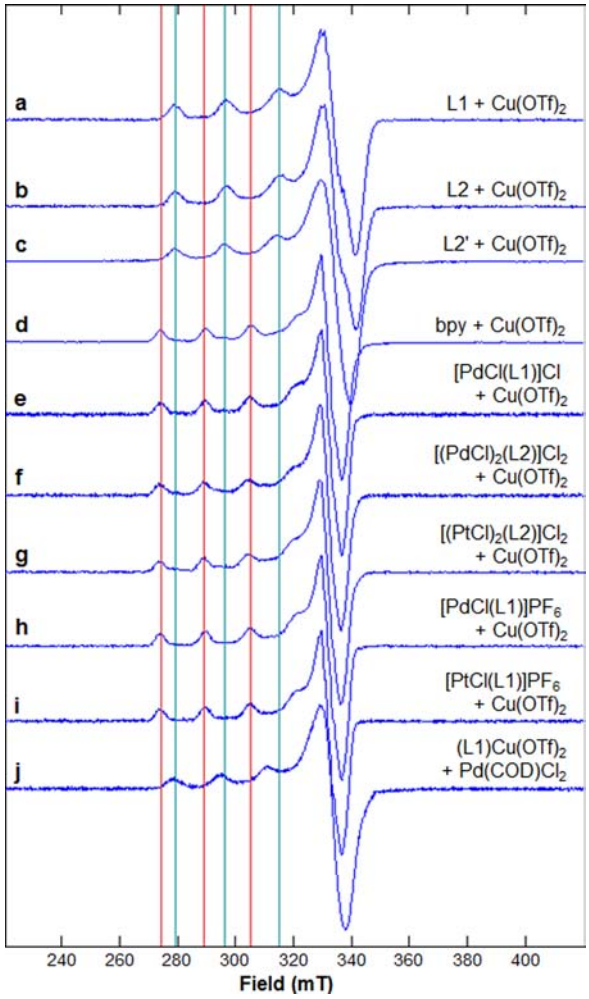

Figure 5. Glass EPR spectra of Cu, Pd/Cu, and Pt/Cu complexes in 50:50 DMSO/H_2O at 20 K. Red and blue lines are to guide the eye.

The addition of 2 equiv of $Cu(OTf)_2$ to L1 in 50:50 DMSO/H_2O results in EPR spectra exhibiting eight lines in the parallel region rather than the four observed in monometallic Cu^{2+} complexes (see the spectrum in the Supporting Information). This doubling of the hyperfine lines is consistent with a coupling between two Cu^{2+} centers separated by a fixed distance.[36−39] On the basis of a simple molecular model using Spartan,[40] the estimated distance between these two sites is ca. 8 Å. Simulation of the spectrum yielded the following EPR parameters: $g_\parallel = 2.38$, $g_\perp = 2.07$, $A_\parallel = 160 \times 10^{-4}$ cm^{-1}, and $A_\perp = 39 \times 10^{-4}$ cm^{-1}. The minimum exchange coupling that could be used to achieve the best fit for this simulation was 2×10^4 MHz, and this value falls well within the range of couplings for related dinuclear Cu^{2+} species.[36−39] An additional half-field

dx.doi.org/10.1021/ic401952s | Inorg. Chem. 2013, 52, 14116−14123

signal for the spin-forbidden $\Delta M_s = 2$ transition between $M_s = \pm 1$ was also observed, giving further confirmation of a coupling interaction between two Cu^{2+} centers.

Rh/Cu Complexes. The differing binding selectivities of Rh and Cu for the bpy and dpa sites within L1 and L2 suggest that Rh/Cu complexes of L1 and L2 should be readily accessible by both routes in Figure 6. A rust-colored product is obtained upon reaction of 1 equiv of $Cu(OTf)_2$ with [Rh(COD)(L1)]-Cl. An identical product with a matching IR spectrum can be obtained from the reaction of 0.5 equiv of $[Rh(COD)Cl]_2$ with a freshly prepared solution of L1 and $Cu(OTf)_2$ in a 1:1 ratio. Very similar IR spectra can also be obtained for the brown products of analogous L2 reactions involving 1:1:2 ratios of L2 to Rh to Cu using the same Rh and Cu sources. EPR spectra of the complexes in CH_3OH are also unaffected by the order of metal addition and indicate the presence of only one type of Cu^{2+} center (Figure 7). The EPR parameters obtained from these spectra are very similar to those of the bpy and dpa $Cu(OTf)_2$ complexes, with the $A_{\|}$ values being more consistent with those of the dpa complexes (Table 2). EPR of these complexes using 50:50 DMSO/H_2O was not possible because DMSO is known to readily replace COD on Rh complexes.[41] The compositions of the products **1** and **2** were confirmed by elemental analysis, and the $[M - OTf]^+$ ion for complex **1** was observed by electrospray ionization mass spectrometry (ESI-MS).

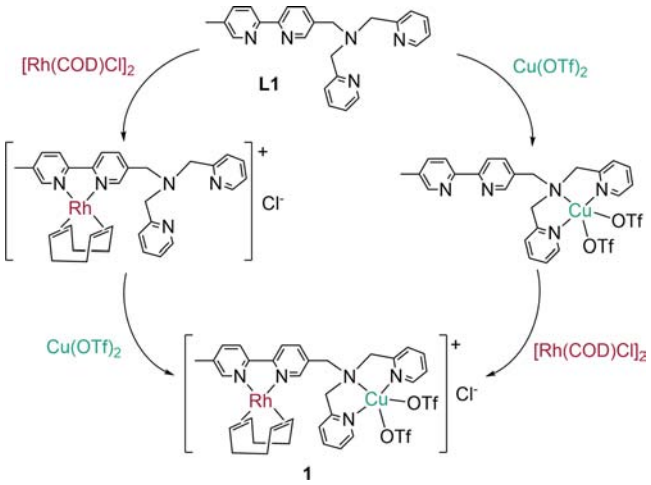

Figure 6. Complementary routes for the synthesis of **1**. The synthesis of **2** is analogous.

Pd/Cu and Pt/Cu Complexes. In 50:50 DMSO/H_2O, the glass EPR spectra of 1:1 mixtures of $Cu(OTf)_2$ with various L1 and L2 complexes of Pd^{2+} or Pt^{2+} were recorded (Table 3). In contrast to the results for mixtures of $Cu(OTf)_2$ with the ligands alone, the resulting EPR parameters match those of the bpy0 case rather than those of L2′ (Figure 5c–i). This is an expected result based on Scheme 2, with the dpa-selective Cu^{2+} binding at the bpy site because the dpa site is blocked by the already-bound Pd^{2+} or Pt^{2+}, resulting in the formation of complexes **3**–**5**, $[Cu(OTf)_2(L1)PdCl]PF_6$ (**5′**), and $[Cu(OTf)_2(L1)PtCl]PF_6$ (**7**) (Figure 8). The addition of more than 1 equiv of $Cu(OTf)_2$ to these solutions of Pd and Pt complexes of L1 and L2 does not lead to replacement of the Pd or Pt centers by Cu. Instead, the same **3**–**5** and **7** products are observed as mixtures with free $Cu(OTf)_2$. Despite changes in the metal (Pt^{2+} or Pd^{2+}), ligand (L1 or L2), and counterion (PF_6^- or Cl^-), all of the EPR spectra of complexes **3**–**5** and **7** are essentially superimposable.

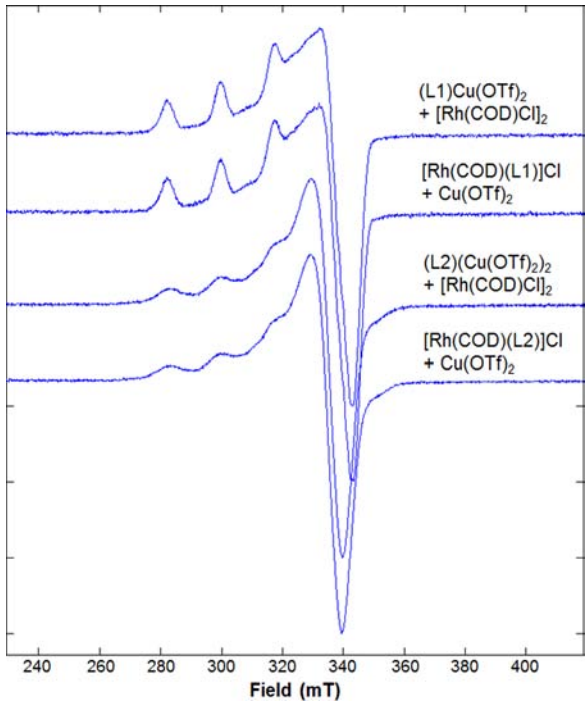

Figure 7. EPR spectra of the samples obtained from different routes of synthesizing **1** and **2**.

Table 2. EPR Data for Rh/Cu Complexes in MeOH at 20 K

entry	complex	$g_{\|}$	$g_{\perp}$	$A_{\|}$ ($\times 10^{-4}$ cm^{-1})
1	**1**	2.23	2.05	179
2	**2**	2.23	2.06	179

Pd/Cu and Pt/Cu L2 complexes **3** and **4** can be easily isolated and purified by reaction in CH_3OH because the mint-green products precipitate from the reaction mixture. The same products are produced from 1:1.1 and 1:2 mixtures of the Pd or Pt L2 complexes with $Cu(OTf)_2$, confirming that Cu^{2+} does not exchange with Pd^{2+}. The slightly darker mint-green L1 product **5** can also be obtained from a 1:1 mixture of [PdCl(L1)]Cl with $Cu(OTf)_2$ in methanol by precipitation with diethyl ether. When Cu^{2+} is first allowed to react with L1 in methanol followed by the addition of $Pd(COD)Cl_2$, a grayish-teal precipitate begins to form within 5 min (Figure 9). The product **6**, which clearly has different physical properties than **5**, also has a different EPR spectrum (Figure 5j), which more closely corresponds to dpa-bound Cu^{2+} than bpy-bound Cu^{2+}. The compositions of the isolated Pd/Cu and Pt/Cu complexes **3**–**6** were confirmed by elemental analysis. For complex **6**, the binding of both Cu and Pd to L1 was confirmed by the presence of signals for $[(L1)CuPdCl_2]^{2+}$, $[(L1)CuPd(OTf)Cl]^{2+}$, and $[(L1)CuPd(OTf)Cl_2]^+$ in the mass spectrum, although none of these ions contains both of the $(L1)Cu(OTf)_2$ moieties proposed. Multiple ions corresponding to complexes **3**–**5** with loss of Cl^- and/or OTf^- ions were observed in their mass spectra. Note that all of these compounds have been drawn as though each metal retains its original ancillary ligands, but exchange of the chloride and triflate ions either during synthesis or under the ESI-MS conditions cannot be ruled out.

dx.doi.org/10.1021/ic401952s | Inorg. Chem. 2013, 52, 14116–14123

Table 3. EPR Data Obtained for Pd/Cu and Pt/Cu Complexes in 50:50 DMSO/H_2O at 20 K

entry	ligand	first metal added	second metal added	counterion	product	$g_{\|}$	$g_{\perp}$	$A_{\|}$ (10^{-4} cm^{-1})
1	L1	Pd	Cu	Cl^-	**5**	2.31	2.07	163
2	L2	Pd	Cu	Cl^-	**3**	2.32	2.07	161
3	L2	Pt	Cu	Cl^-	**4**	2.32	2.07	161
4	L1	Pd	Cu	PF_6^-	**5′**	2.31	2.07	163
5	L1	Pt	Cu	PF_6^-	**7**	2.31	2.07	163
6	L1	Cu	Pd	Cl^-	**6**	2.27	2.07	168

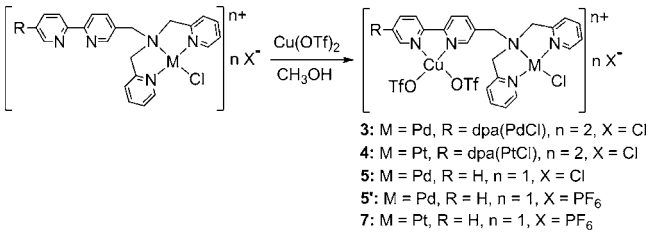

3: M = Pd, R = dpa(PdCl), n = 2, X = Cl
4: M = Pt, R = dpa(PtCl), n = 2, X = Cl
5: M = Pd, R = H, n = 1, X = Cl
5′: M = Pd, R = H, n = 1, X = PF_6
7: M = Pt, R = H, n = 1, X = PF_6

Figure 8. Reaction of Pd and Pt complexes with $Cu(OTf)_2$.

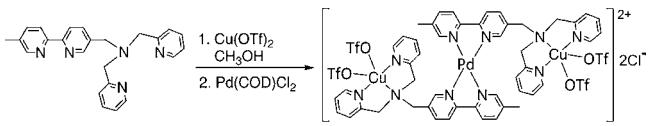

6

Figure 9. Synthesis of Pd/Cu complex **6** with bpy-bound Pd and dpa-bound Cu.

CONCLUSIONS

The viability of IR, one of the simplest characterization techniques, to make the distinction between metal-binding preferences to two similar polypyridyl-based sites in bpy−dpa ligands was demonstrated for the paramagnetic metals Cu^{2+} and Co^{2+}. Preference for dpa binding was observed for both of these metals, which was particularly interesting for Co^{2+}, whose binding selectivity in bpy−dpa complexes had not been previously explored. EPR data for Cu^{2+} complexes were also consistent with dpa selectivity. The opposing site selectivities of Rh^+ and Cu^{2+} for bpy and dpa, respectively, allowed for the formation of Rh/Cu heterometallic complexes by routes involving either order of metal addition. In contrast, for the production of heterometallic Pd/Cu and Pt/Cu complexes in which both metals have identical dpa site selectivities, the order of metal addition could be used to control the regiochemistry of metalation. EPR could be used to determine the final placement of Cu^{2+} in these Pd/Cu and Pt/Cu heterometallic complexes despite the similarity of the two sites. These results provide a method for determining the binding site of paramagnetic metals in heterometallic complexes of bpy−dpa ligands, extending the useful range of metals for which these ligands can be used. It is expected that these characterization techniques as well as the knowledge of these specific metal-binding selectivities can be applied toward the straightforward and controllable synthesis of a wide array of tunable heterometallic complexes involving related multisite polypyridyl ligands.

ASSOCIATED CONTENT

Supporting Information

Synthetic procedures for $(L1)Cu(OTf)_2$ and $(L2)(Cu(OTf)_2)_2$, table of selected data obtained in IR studies, comparison of IR data for Rh/Cu complexes obtained from both routes, examples of simulated EPR spectra, and a half-field EPR spectrum of a 2:1 mixture of $Cu(OTf)_2$ and L1. This material is available free of charge via the Internet at http://pubs.acs.org.

AUTHOR INFORMATION

Corresponding Author

*E-mail: lmwhite@chem.ufl.edu.

Notes

The authors declare no competing financial interest.

ACKNOWLEDGMENTS

Fellowship support was provided for S.K.G. by the University of Florida through the Alumni Fellowship program. Funding for the undergraduate research of R.C.W. was provided through the UF HHMI Science for Life program. We thank Lukas Hibell for assistance with preparation of the starting materials.

REFERENCES

(1) Van Den Beuken, E. K.; Feringa, B. L. *Tetrahedron* **1998**, *54*, 12985.
(2) *Catalysis by Di- and Polynuclear Metal Cluster Complexes*; Adams, R. D., Cotton, F. A., Eds.; Wiley-VCH: New York, 1998.
(3) Braunstein, P.; Rosé, J. In *Metal Clusters in Chemistry*; Braunstein, P., Oro, L. A., Raithby, P. R., Eds.; Wiley-VCH: Weinheim, Germany, 1999; Vol. 2, p 616.
(4) Stephan, D. W. *Coord. Chem. Rev.* **1989**, *95*, 41.
(5) Wheatley, N.; Kalck, P. *Chem. Rev.* **1999**, *99*, 3379.
(6) Cooper, B. G.; Napoline, J. W.; Thomas, C. M. *Catal. Rev.: Sci. Eng.* **2012**, *54*, 1.
(7) Inagaki, A.; Edure, S.; Yatsuda, S.; Akita, M. *Chem. Commun.* **2005**, *0*, 5468.
(8) Hidai, M.; Matsuzaka, H. *Polyhedron* **1988**, *7*, 2369.
(9) Tsukada, N.; Ohnishi, N.; Aono, S.; Takahashi, F. *Organometallics* **2012**, *31*, 7336.
(10) Karshtedt, D.; Bell, A. T.; Tilley, T. D. *Organometallics* **2003**, *22*, 2855.
(11) Gu, S.; Xu, D.; Chen, W. *Dalton Trans.* **2011**, *40*, 1576.
(12) Suess, D. L. M.; Peters, J. C. *Chem. Commun.* **2010**, *46*, 6554.
(13) Fordyce, W. A.; Pool, K. H.; Crosby, G. A. *Inorg. Chem.* **1982**, *21*, 1027.
(14) Guha, P. M.; Phan, H.; Kinyon, J. S.; Brotherton, W. S.; Sreenath, K.; Simmons, J. T.; Wang, Z.; Clark, R. J.; Dalal, N. S.; Shatruk, M.; Zhu, L. *Inorg. Chem.* **2012**, *51*, 3465.
(15) Moret, M.-E.; Chen, P. *Organometallics* **2008**, *27*, 4903.
(16) Takebayashi, S.; Ikeda, M.; Takeuchi, M.; Shinkai, S. *Chem. Commun.* **2004**, 420.
(17) Takebayashi, S.; Shinkai, S.; Ikeda, M.; Takeuchi, M. *Org. Biomol. Chem.* **2008**, *6*, 493.
(18) Zhang, L.; Clark, R. J.; Zhu, L. *Chem.—Eur. J.* **2008**, *14*, 2894.
(19) Araya, J. C.; Gajardo, J.; Moya, S. A.; Aguirre, P.; Toupet, L.; Williams, J. A. G.; Escadeillas, M.; Le Bozec, H.; Guerchais, V. *New J. Chem.* **2010**, *34*, 21.
(20) Lee, P. K.; Law, W. H. T.; Liu, H. W.; Lo, K. K. W. *Inorg. Chem.* **2011**, *50*, 8570.
(21) Goforth, S. K.; Walroth, R. C.; McElwee-White, L. *Inorg. Chem.* **2013**, *52*, 5692.

(22) Son, K.-s.; Pearson, D. M.; Jeon, S.-J.; Waymouth, R. M. *Eur. J. Inorg. Chem.* **2011**, *2011*, 4256.
(23) Baudot, A.; Alger, L.; Boutron, P. *Cryobiology* **2000**, *40*, 151.
(24) Doba, T.; Ingold, K. U.; Reddoch, A. H.; Siebrand, W.; Wildman, T. A. *J. Chem. Phys.* **1987**, *86*, 6622.
(25) Stoll, S.; Schweiger, A. *J. Magn. Reson.* **2006**, *178*, 42.
(26) Nanthakumar, A.; Fox, S.; Murthy, N. N.; Karlin, K. D. *J. Am. Chem. Soc.* **1997**, *119*, 3898.
(27) Kooistra, T. M.; Hekking, K. F. W.; Knijnenburg, Q.; Bruin, B. d.; Budzelaar, P. H. M.; Gelder, R. d.; Smits, J. M. M.; Gal, A. W. *Eur. J. Inorg. Chem.* **2003**, 648.
(28) Tamamura, H.; Ojida, A.; Ogawa, T.; Tsutsumi, H.; Masuno, H.; Nakashima, H.; Yamamoto, N.; Hamachi, I.; Fujii, N. *J. Med. Chem.* **2006**, *49*, 3412.
(29) Kawahara, S.-i.; Uchimaru, T. *Eur. J. Inorg. Chem.* **2001**, 2437.
(30) Storr, T.; Sugai, Y.; Barta, C. A.; Mikata, Y.; Adam, M. J.; Yano, S.; Orvig, C. *Inorg. Chem.* **2005**, *44*, 2698.
(31) Gerasimova, T. P.; Katsyuba, S. A. *Dalton Trans.* **2013**, *42*, 1787.
(32) Ibrahim, M. M. *J. Mol. Struct.* **2011**, *990*, 227.
(33) Kim, M.; Mora, C.; Lee, Y. H.; Clegg, J. K.; Lindoy, L. F.; Min, K. S.; Thuéry, P.; Kim, Y. *Inorg. Chem. Commun.* **2010**, *13*, 1148.
(34) Niklas, N.; Alsfasser, R. *Dalton Trans.* **2006**, 3188.
(35) Zanardi, A.; Corberán, R.; Mata, J. A.; Peris, E. *Organometallics* **2008**, *27*, 3570.
(36) Bernhardt, P. V. *Inorg. Chem.* **2001**, *40*, 1086.
(37) Ainscough, E. W.; Brodie, A. M.; Davidson, R. J.; Moubaraki, B.; Murray, K. S.; Otter, C. A.; Waterland, M. R. *Inorg. Chem.* **2008**, *47*, 9182.
(38) Pierpont, C. G.; Francesconi, L. C.; Hendrickson, D. N. *Inorg. Chem.* **1978**, *17*, 3470.
(39) Klingele, J.; Moubaraki, B.; Murray, K. S.; Boas, J. F.; Brooker, S. *Eur. J. Inorg. Chem.* **2005**, *2005*, 1530.
(40) *Spartan '10*; Wavefunction Inc.: Irvine, CA, 2010.
(41) Dorta, R.; Rozenberg, H.; Shimon, L. J. W.; Milstein, D. *Chem.—Eur. J.* **2003**, *9*, 5237.